Structural Chemistry (2022) 33:1241–1250
https://doi.org/10.1007/s11224-022-01929-9

ORIGINAL RESEARCH

Investigation of structural, electronic, and antioxidant properties of calycopetrin and xanthomicrol as two polymethoxylated flavones using DFT calculations

Arjang Jalezadeh[1] · Zohreh Mirjafary[1] · Morteza Rouhani[1] · Hamid Saeidian[2]

Received: 7 March 2022 / Accepted: 31 March 2022 / Published online: 11 April 2022

Abstract
Calycopetrin (Cal) and xanthomicrol (Xan) are extracted from various plant sources as polymethoxylated flavones and have extraordinary biological properties. All structural, electronic, and spectral data of these two compounds such as HOMO, LUMO energies, electrophilicity index, molecular electrostatic potential maps, ^{1}HNMR, and ^{13}CNMR were obtained using B3LYP/6–31 + G(d, p) computational method and were examined and interpreted in detail. Their antioxidant properties were also evaluated by hydrogen atom transfer, single electron transfer followed by proton transfer, and the sequential proton loss electron transfer mechanisms in the gas phase and water and compared with phenol. Delocalization of odd electrons in the studied radicals was also investigated using spin density maps. Finally, the reactivity of Cal and Xan with oxygen radicals such as HO˙, HOO˙, and $O_2^{\cdot -}$ was investigated.

Keywords Calycopetrin · Xanthomicrol · Antioxidant · DFT calculation · Aromaticity

Introduction

Flavonoids and polyphenols have great potential to treat a variety of cancers [1–5]. A subset of these compounds are flavonoids whose hydroxy groups are methylated and this increases metabolic stability and thus improves their biological properties [6, 7]. Calycopetrin and xanthomicrol (hereinafter referred to as "Cal" and "Xan," respectively) are two examples of these compounds. Cal, (5, 4'- dihydroxy-3,6,7,8-tetramethoxyflavone) is a flavonoid first extracted and identified from leaves of *Calycopteris floribunda* Lamk. and *Digitalis thapsi* [8, 9]. Many biological properties have been reported for Cal, including immunoinhibitory, anti-helminthic, anti-spasmodic, and hyperlipidemic agents [10, 11]. The effect of this compound on the treatment of neurodegenerative diseases and rheumatoid diseases such as Alzheimer's and cancer diseases has also been studied and good results have been obtained [12, 13]. Xan (5, 4 '-dihydroxy-6,7,8-trimethoxyflavone), like Cal, is a methoxylated flavonoid found in the leaves of various plants, including Dracocephalum kotschyi Boiss [14]. Unique biological properties such as anti-cancer and anti-angiogenic properties have been reported for this compound [15–18].

Free radicals are highly active and reactive due to the unpaired electrons of the species. Free radicals in the body are created by the activity of various parts and compounds. These include the activity of mitochondrion and phospholipase enzymes. In addition, the human body can be exposed to other types of free radicals from various environmental sources such as cigarette smoke or air pollution. Free radicals can damage cells through oxidative stress. On the other hand, free radicals have vital functions in the body, including fighting infectious agents to boost the immune system. For this reason, the body needs to balance the required free radicals with antioxidants [19–21].

Antioxidants are compounds that inhibit oxidation in the body's cells through various mechanisms. An antioxidant usually acts through the chemical mechanism of hydrogen atom transfer (HAT) and single electron transfer followed by proton transfer (SET-PT) [22, 23]. In the first mechanism, a free radical receives hydrogen from the antioxidant and the antioxidant is transformed into a stable radical. In this mechanism, bond

✉ Zohreh Mirjafary
zmirjafary@srbiau.ac.ir

✉ Hamid Saeidian
Saeidian1980@gmail.com

[1] Department of Chemistry, Science and Research Branch, Islamic Azad University, Tehran, Iran

[2] Department of Science, Payame Noor University (PNU), P.O. Box, 19395-3697 Tehran, Iran

dissociation energy (BDE) for the O–H bond is an important parameter for evaluating antioxidant activity so that the weaker O–H bond shows strong antioxidant properties and vice versa [24, 25]. In the SET-PT mechanism, the antioxidant compound can give an electron to a free radical and turn itself into a radical cation. In this mechanism, ionization potential energy (IP) is discussed so a combination with lower IP should have more robust antioxidant properties [26, 27]. Two of the most important natural and non-enzymatic antioxidants are phenolic and flavonoid compounds [28–30]. Cal and Xan can be expected to have good antioxidant properties. The rapid and reliable development of quantum chemistry allows the calculations of BDEs and IPs of organic compounds to be obtained with great accuracy. Density functional theory (DFT) calculations methods can be used as a powerful tool to predict the relationship between chemical structure and the activity of an organic compound [31, 32]. Numerous quantum studies have been conducted to investigate the antioxidant properties and design new compounds as antioxidants [33–40]. Scientific sources indicate that no DFT studies have been performed to obtain Cal and Xan flavonoids physico-chemical properties. In the present work, the structure of these two valuable flavonoids was comprehensively considered to obtain antioxidant capacity, acidity, electronic, and structural and spectral data using the DFT method. Their structures consist of a polymethoxylated phenol ring A and a fused γ-pyrone ring C, with the phenol ring B attached to the 2-position of the γ-pyrone ring.

Computational details

The chemical structures of Cal and Xan, their anions, radicals, and radical cations were optimized using the DFT/B3LYP method in conjunction with basis set 6–31 + G(d, p) using Gaussian 09 software [41]. The unrestricted open-shell method was used to optimize radical and radical cation species. Vibrational frequencies were calculated at the same level to ensure that each stationary point is a real minimum. All calculations were performed in the gas phase and water. We have employed solvent effects into account by using the conductor-like polarizable continuum model (CPCM). The B3LYP/6–31 + G (d, p) optimized Cartesian coordinates of Cal and Xan, their anions, radicals, and radical cations have been collected in the Supplementary material.

Results and discussion

Benchmarking study of computational method

The DFT method is a valuable and powerful computational method because it predicts the physical and chemical data of the studied system with high accuracy. Nowadays, DFT/B3LYP method is widely used for various quantum computations [42–48]. This method was used with the basis set 6–31 + G(d, p) to study the Cal and Xan structures in the present study. Spectral data (^{1}HNMR and ^{13}CNMR) of Cal have been reported experimentally [10]. These data can be used to benchmark the computational method B3LYP/6–31 + G(d, p). Given that NMR data were obtained in acetone-d_6 as a solvent, the structure of Cal in this solvent was also optimized using the conductor-like polarizable continuum model (CPCM) as the solvation model [49]. Spectral data (regarding hydrogens and carbons of tetramethylsilane) were obtained by the gauge-independent atomic orbital (GIAO) method [50] in acetone. Experimental and computational NMR data of Cal have been collected in Table 1S (supplementary material).

As can be seen from the ^{1}HNMR and ^{13}CNMR data regression curves (Fig. 1), there is an excellent agreement between the experimental and calculated data; regression was obtained $R^2 = 0.9964$ for ^{1}HNMR and $R^2 = 0.9966$ for ^{13}CNMR data. Therefore, the computational method of B3LYP/6–31 + G(d, p) can be used to continue the calculations and obtain the physical and chemical properties of Cal and Xan flavonoids.

Structural characterization of Cal and Xan

The Cal and Xan structures optimized using the B3LYP/6–31 + G(d, p) method have been shown in Fig. 2. Some structural data of the studied compounds are tabulated in Table 1.

As can be seen from the optimized structure of the molecules, all three polymethoxylated phenyl (A) phenolic (B), and γ-pyrone (C) rings are almost in the same plane, and the molecules are in an extended conjugation system that can be viewed from dihedral angles. The angle of ^{17}C–^{9}C–^{8}C–^{7}C in Cal is 179.07° and the ^{16}C–^{9}C–^{8}C–^{7}C in Xan is 179.91°. The bond length of C = O in Xan and Cal is 1.262 and 1.264 Å, respectively, which is longer than the bond length of a group of a normal ketone. On the other hand, the calculated vibration frequency of the carbonyl group in Cal and Xan is 1670 and 1673 cm^{-1}, respectively, which is much lower than the frequency of a normal ketone group (1715 cm^{-1}). The carbonyl group can be conjugated with the endo alkene double bond and the endo-oxygen atom. This phenomenon decreases the bond order of the carbonyl bond and makes it more single. In the resonance form, the γ-pyrone core is an aromatic ring. The presence of intramolecular hydrogen bonding (IMHB) increases the tendency for this resonance (Scheme 1).

As can be seen from the optimized structures of Cal and Xan (Fig. 2), there is a very strong IMHB with the hydrogen atom of the hydroxy group as the donor center and the oxygen atom of the carbonyl group as the acceptor site. In

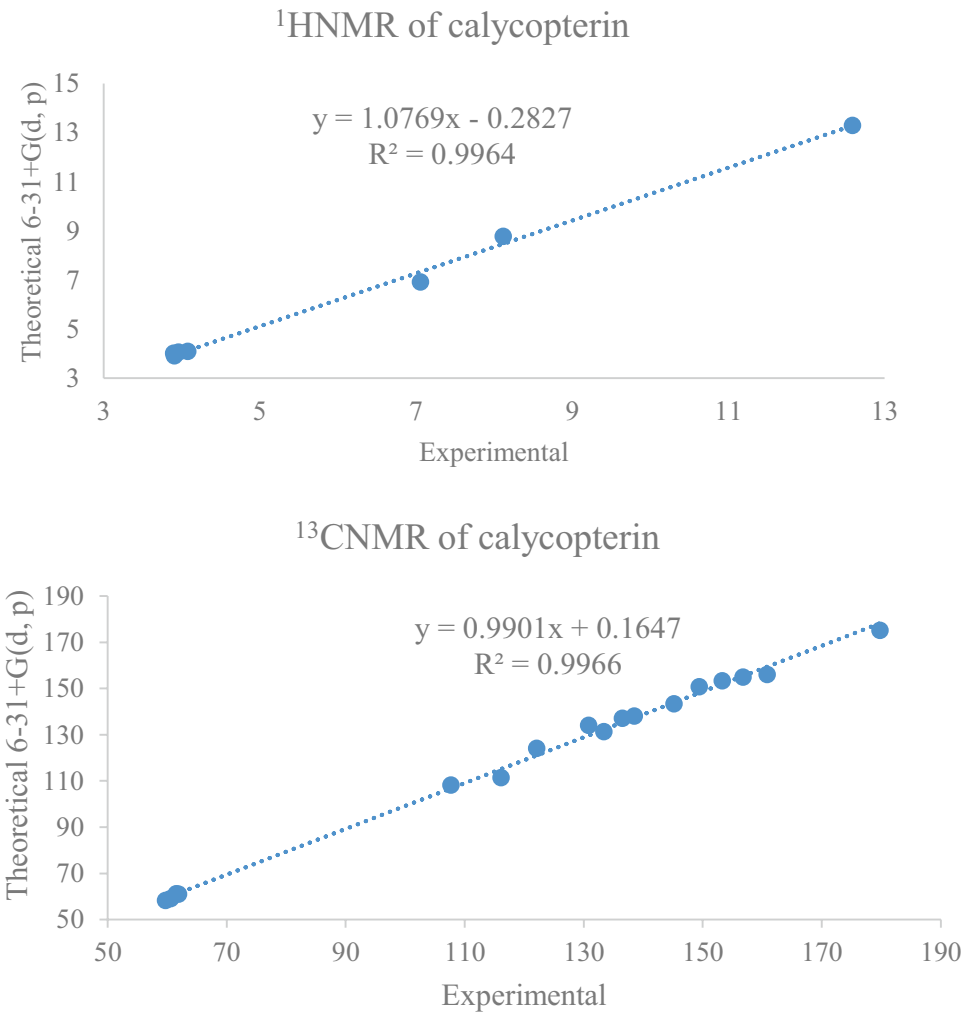

Fig. 1 The linear regression between experimental and calculated ^{1}H and ^{13}CNMR data of calycopterin

the section on evaluating the antioxidant properties of the studied compounds, we will see how this IMHB will affect these properties. Calculation of γ-pyrone ring aromatics indices using the B3LYP/6–31 + G(d, p) method can confirm the existence of this resonance form. The Harmonic Oscillator Model of Aromaticity (HOMA) and the Nucleus-Independent Chemical Shifts (NICS) are two structural and magnetic aromatics indices widely used today to evaluate the aromaticity of unsaturated system rings [51, 52]. The HOMA index is used to evaluate all carbon systems such as hydrocarbons. The Harmonic oscillator model of electron delocalization (HOMED) is used to evaluate the aromaticity of rings containing heteroatoms such as the pyrone ring (Eq. (1)) [53, 54].

$$\text{HOMA or HOMED} = 1 - \left(\sum \alpha \sum [R_{opt} - R_x]^2\right)/n \quad (1)$$

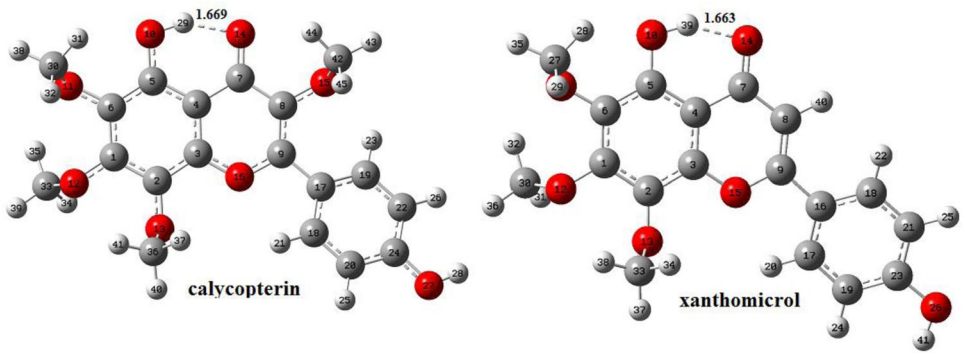

Fig. 2 The B3LYP/6–31 + G(d, p) optimized geometry of calycopterin and xanthomicrol in water (distance in Å)

Table 1 The calculated structural data and aromatic indices of calycopterin and xanthomicrol by B3LYP/6–31 + G(d, p) method

Parameter	Value[a]	
	Calycopterin	Xanthomicrol
IMHB[b] length (Å)	1.669 (1.675)	1.663 (1.672)
IMHB angle (°)	150.25 (149.47)	150.61 (149.76)
C = O bond length (Å)	1.262 (1.256)	1.264 (1.255)
C_B–C_C bond length[c] (Å)	1.469 (1.471)	1.467 (1.470)
C = O stretching frequency (cm^{-1})	1670 (1679)	1673 (1689)
HOMA[d]	0.72 (0.73)	0.71 (0.74)
$NICS_{zz}(1)$[e] (ppm)	-4.91 (-2.14)	-3.68 (-1.87)

[a]In parenthesis for the gas phase

[b]IMHB: intramolecular hydrogen bond

[c]bond between rings B and C

[d]Harmonic oscillator model of aromaticity for γ-pyrone ring C

[e]Nucleus-independent chemical shifts for γ-pyrone ring C ($NICS_{zz}$) calculated at GIAO-B3LYP/6–31 + G(d, p) level

In this equation, the parameters n, α, R_{opt} and R_x are the number of bonds within the ring, the normalization constant, the optimized bond length for the reference molecule, and the calculated bond length for the study ring, respectively. HOMED is equal to unity for the benzene ring. It should be noted that α and R_{opt} are different for different types of bonds. In this study, for the C–C bond, R_{opt} and α were equal to 1.394 and 88.09 Å, respectively, and for C–O, R_{opt}, and α were 1.281 and 75.00 Å, respectively [53]. In addition to the HOMA index, the magnetic susceptibility of the ring is an indicator of its aromatic properties, which can be measured by the NICS descriptor [55]. The absolute magnetic shielding is measured using the hypothetical Bq atom at a distance of 1 Å above the ring. Negative and positive NICS values indicate aromaticity and anti-aromaticity, respectively. The HOMA parameters in water for the γ-pyrone ring in Cal and Xan are 0.72 and 0.71, respectively, indicating its aromatic nature. Also, the NICS value of this ring in Cal and Xan in water is 4.91 and 3.68 ppm, respectively, which confirms its relative aromaticity. The same trend is also seen in the gas phase (Table 1). Molecular electrostatic potential (MEP) maps for Cal and Xan also confirm the γ-pyrone aromaticity and the negative charge on the carbonyl oxygen atom. In these maps, red indicates negative electron density and blue indicates positive electron density [56] (Fig. 1S, supplementary material).

The resonance form and IMHB for Cal and Xan can be better investigated by natural bond orbital (NBO). NBO analysis gives numerically the valuable information about intermolecular and intramolecular interactions such as hydrogen bonding and delocalization according to the second-order perturbation energy ($E^{(2)}$). The NBO analysis is a useful method for the study of the charge transfer in a chemical system [57]. Significant intramolecular interactions and $E^{(2)}$ in Cal and Xan structures were collected in Table 2. It should be mentioned that the $E^{(2)}$ value demonstrates the electron transfer from the donor NBOs to acceptors ones.

As seen from Table 2, the LP (2) O14 → BD*(1) O10 H29 as a remarkable interaction with energy 25.91 kcal/mol in Cal structure is attributed to the IMHB interaction. The energy of intramolecular hydrogen interaction in Xan molecule is 26.97 kcal/mol. Moreover, the BD (2) C8–C9 → BD*(2) C7–O14 and LP (2) O15 → BD*(2) C8–C9 in Cal show other significant interactions with 25.57 and 31.77 kcal/mol, respectively. The analogous trend can be seen in the Xan system (Table 2). Such interactions were a consequence of π-bond delocalization and aromaticity of γ-pyrone ring (Scheme 1) which demonstrates a significant ring current. Such findings confirm that the strongest interactions in Cal and Xan structure are related to the IMHB, aromaticity, and conjugation.

Electronic characterization of Cal and Xan

Electronic data calculated by B3LYP/6–31 G + (d, p) method for Cal and Xan have been collected in Table 3. The Cal and Xan dipole moments in water are 6.46 and 8.50 Debye, respectively, indicating the high polarity. The presence of polar groups such as the carbonyl group and the assumed resonance form (Scheme 1) is the reasons for this high dipolar moment value. A noteworthy point is the high polarity of

Scheme 1 Resonance form of calycopterin

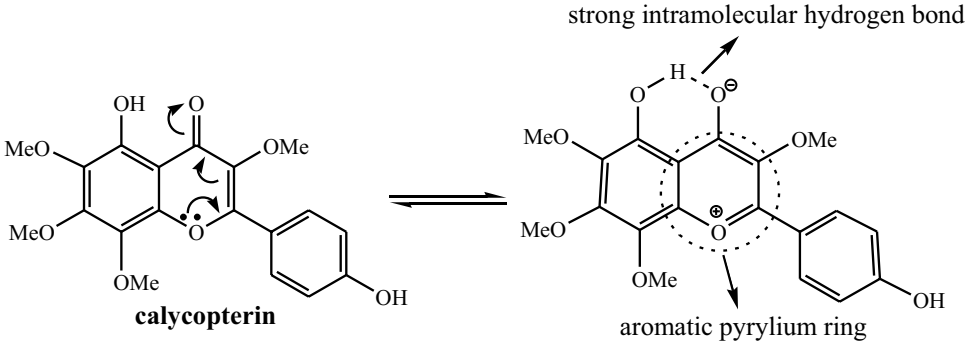

Table 2 Representative calculated donor–acceptor interactions in Cal and Xan at B3LYP/6–31 + G (d,p) level

Structure	Donor NBO (i)	Acceptor NBO (j)	E^2 (kcal/mol)
Calycopterin	BD (2) C8–C9	BD*(2) C7–O14	25.57
	LP (2) O14	BD*(1) O10–H29	25.91
	LP (2) O16	BD*(2) C8–C9	31.77
Xanthomicrol	BD (2) C8–C9	BD*(2) C7–O14	26.07
	LP (2) O14	BD*(1) O10–H39	26.97
	LP (2) O15	BD*(2) C8–C9	33.74

[a]For numbering of atoms, refer to Fig. 2

these compounds in the polar solvent such as water relative to the gas phase (Table 3).

According to Frontier molecular orbital theory, the highest occupied molecular orbital (HOMO) and the lowest unoccupied molecular orbital (LUMO) are usually involved in chemical reactions. In terms of energy, it is easier to separate electrons from HOMO, and this orbital can donate electrons, while LUMO accepts electrons more easily. The geometric shape of the frontier molecular orbitals for Cal and Xan was obtained through the B3LYP/6–31 + G(d, p) method. As shown in Fig. 3, HOMO in both compounds is essentially present in the entire chemical structure. LUMO is present in both compounds on polar groups such as carbonyl and alkene double bond. In general, LUMO is located on A and C rings. HOMO energy measures radical scavenging activity through its electron donation ability to free radical electrons [33]. Calculations show that the HOMO energy level in Cal is higher than in Xan. Therefore, it is suggested that the ability of radical scavenging of Cal is higher than Xan, which will be explained in detail in the section on the antioxidant properties of these compounds. Also, the difference between HOMA and LUMO energy levels (E_g) for Cal and Xan is 3.82 and 3.91 eV, respectively (Fig. 3).

Table 3 The calculated electronic data of calycopterin and xanthomicrol by B3LYP/6–31 + G(d, p) method

Parameter	Value[a]	
	Calycopterin	Xanthomicrol
μ_D (Debye)	6.46 (3.69)	8.50 (5.58)
E_g (E_{LUMO}- E_{HOMO}) (eV)	3.82 (3.71)	3.91 (3.80)
Ionisation potential (I=-E_{HOMO}) (eV)	6.11 (5.84)	6.20 (5.94)
Electron affinity (A=-E_{LUMO}) (eV)	2.29 (2.13)	2.29 (2.14)
Chemical potential (μ=-(I+A)/2) (eV)	4.20 (3.98)	4.24 (4.04)
Chemical hardness (η=(IA)/2 (eV)	1.91 (1.85)	1.95 (1.90)
Electrophilicity (ω=μ^2/2 η) (eV)	4.61 (4.28)	4.60 (4.29)
Nucleophilicity (N=E_{HOMO} (Nu)—E_{HOMO} (TCE)[b]) (eV)	2.88 (3.57)	2.79 (3.47)
Log P_O/P_W=-ΔG/2.303RT[c]	1.10	1.09

[a]In parenthesis for the gas phase

[b]E_{HOMO} of tetracyanoethylene

[c]partition coefficient between *n*-octanol and water

General reactivity indices including chemical potential (μ), chemical hardness (η), global electrophilicity (ω), and global nucleophilicity (N) were calculated for both Cal and Xan flavonoids using the B3LYP/6–31 + G(d, p) (Table 3) method [58, 59]. Chemical hardness, which indicates the resistance of cloud polarization or deformation of chemical compounds, is used to predict reactivity. According to the chemical hardness of Cal and Xan, it seems that Cal has higher reactivity than Xan because it has a lower chemical hardness. Indices ω and N are useful and reliable parameters to determine the electrophilic and nucleophilic nature of organic compounds [60–62]. Organic compounds can be classified on the Domingo scale for ω and N indices [63]. This scale divides electrophiles and nucleophiles into strong, moderate, and weak categories. When ω is higher than 1.5 eV, it is a strong electrophile, in the range 0.8–1.5 eV the electrophile is mild and less than 0.8 eV represents the weak electrophile. Also, a strong nucleophile has a nucleophilicity index above 3 eV, while a moderate nucleophile has an N in the range of 2–3 eV and a weak nucleophile has an N lower than 2 eV. Based on this rating and the data in Table 3, it can be seen that Cal and Xan are both strong electrophiles and moderate nucleophiles. It should be noted that the global nucleophilicity value of a molecule is calculated from the difference of its E_{HOMO} energy with the E_{HOMO} energy of the tetracyanoethylene molecule (TCE). The TCE has the lowest HOMO energy among many organic molecules [64]. The antioxidant activity of an organic molecule depends not only on its chemical properties but also on its ability to penetrate the medium. To prevent peroxidation lipid, an antioxidant must have high lipophilicity. The classical descriptor for lipophilicity can be expressed as the value of Log $P_{o/w}$, where P represents the partition coefficient between n-octanol and water. Log $P_{o/w}$ can be calculated from Eq. (2) where R is the gas constant, T is the system temperature (298.15 K) and ΔG is the difference between the solvation Gibbs energies in water and n-octanol for the study compound [65]. Cal has higher lipophilicity than Xan so that Cal can penetrate the lipid layer better than Xan (Table 3).

$$\text{Log } P_o/P_w = -\Delta G/2.303RT \quad (2)$$

DFT study on antioxidant activity of Cal and Xan

In this section, two antioxidant mechanisms, including hydrogen atom transfer (HAT) and single electron transfer followed by proton transfer (SET-PT) were considered to evaluate the antioxidant properties of Cal and Xan. Bond dissociation enthalpies (BDEs) and ionization potentials (IPs) data were calculated using the B3LYP/6–31 + G(d, p)

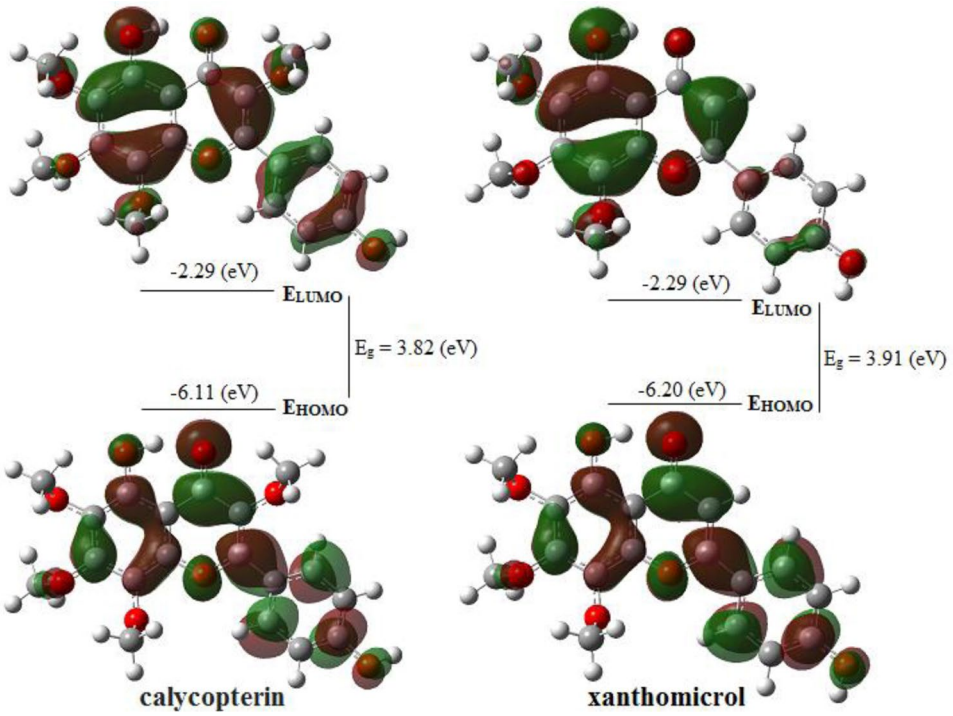

Fig. 3 The HOMO and LUMO gap for calycopterin and xanthomicrol in water

method in the gas phase and water as polar and biological solvent with the CPCM solvation model. In the final step, the reactivity of the studied compounds with the radical species OH°, OOH°, and $O_2^{\circ-}$was also investigated. Reactions ((3) and (4)) related to both mechanisms have been given below [33].

1. Hyrdrogen atom transfer (HAT):

$$R^{\bullet} + ArOH \rightarrow RH + ArO^{\bullet} \quad (3)$$

2. Single electron transfer (HAT):

$$R^{\bullet} + ArOH \rightarrow R^{-} + ArOH^{\bullet+} \rightarrow ArO^{\bullet} + RH \quad (4)$$

As can be deduced from these reactions, these two pathways involve the free radical reaction with the hydroxy group, which can be described by Eqs. (5) and (6):

$$BDE = H_{ArO\cdot} + H_{H\cdot} - H_{ArOH} \quad (5)$$

$$IP = H_{ArO^{\bullet+}} + H_e - H_{ArOH} \quad (6)$$

where $H_{ArO}{}^{\circ}$, $H_{ArO}{}^{\circ+}$, H_{ArOH}, $H_H{}^{\circ}$, and H_e are the enthalpies of radical, radical cation, neutral antioxidant, radical hydrogen, and electron, respectively. $H_H{}^{\circ}$ and H_e in the gas phase and water were extracted from literature [66]. BDEs and IPs data for Cal and Xan were calculated and given in Table 4 and compared to phenol as the reference molecule. In the HAT mechanism, a hydrogen atom from the antioxidant donates to a typical free radical. Therefore, the lower BDE value of the O–H bond represents the higher antioxidant properties. There are two O–H groups in the structure of the studied two flavonoids. Therefore, the BDE of both hydroxy groups is calculated separately. For convenience, the symbols OH_A (on ring A) and OH_B (On ring B) are used to identify radical species.

As can be deduced from the data, the O–H_A bond, energy in Cal and Xan is higher than in phenol and this hydrogen as a radical is not donated to the free radical by

Table 4 B3LYP/6–31 + G(d, p) bond dissociation energies (BDE), ionization potentials (IP), ΔBDE, ΔIP, and proton affinity (PA) values for calycopterin and xanthomicrol[a]

Structure	BDE (kcal/mol)	ΔBDE (kcal/mol)	IP (kcal/mol)	ΔIP (kcal/mol)	PA (kcal/mol)
Phenol	78.75 (80.71)	0	115.86 (188.75)	0	28.81
Cal-OH_A	86.42 (96.44)	7.67 (15.73)	104.46 (160.65)	–11.40 (28.10)	35.96
Cal-OH_B	82.01 (82.78)	3.26 (2.07)	104.46 (160.65)	–11.40 (28.10)	26.34
Xan-OH_A	87.11 (97.80)	8.36 (17.09)	111.44 (163.17)	–4.42 (25.58)	36.48
Xan-OH_B	82.83 (83.72)	4.08 (3.01)	111.44 (163.17)	–4.42 (25.58)	25.40

[a]In parenthesis for the gas phase

these flavonoids. The cause of this phenomenon is due to IMHB, that this atom hydrogen is mainly involved with two oxygen atoms. The hydrogen atom on OH_A is trapped between the two groups through an IMHB. But the BDE of the O–H_B bond is about the same as phenol, and this hydrogen can be released in reaction with a free radical to neutralize the free radical. BDE of this bond in Cal is lower than Xan, so the antioxidant properties of Cal are higher than Xan. Both Cal-OH_A and Cal-OH_B radicals are more stable than Xan-OH_A and Xan-OH_B radicals by amounts of 0.69 and 0.82 kcal/mol, respectively. Cal has an additional methoxide group on the γ-pyrone ring compared to Xan. The methoxy group is considered an electron-donating group. These groups generally reduce the BDE, while the electron-withdrawing groups increase this value. Spin density plots analysis shows that delocalization has occurred for an unpaired electron in OH_B species (Fig. 4). It should be emphasized that unlocalized spin density in the radical leads to the easy formation, so the BDE decreases. By spreading the spin density throughout the molecule, the spin on each atom decreases, resulting in reduced reactivity and increased stability.

The spin density distribution in Cal-OH_B and Xan-OH_B indicates the involvement of ring A and ring C along with α, β unsaturated carbonyl group in unpaired electron delocalization. The spin density plots of radicals show that the pyrone ring plays an important role in the spin distribution and antioxidant properties of the studied compounds. Because free radical scavenging activities always occur in the solvent and because the physiological medium is water, antioxidant calculations in water were also performed. The data in Table 4 show that the BDE of O–H bonds is not highly solvent-dependent. A closer look at the BDE data in the gas phase and water reveals a very valuable point. The dissociation energy of OH_B bonds in the gas and aqueous phases is slightly different from 0.77 kcal/mol for Cal and 0.89 kcal/mol for Xan, which completely agrees with the above findings. But the difference is more remarkable for cleaving the OH_A bond involved with the IMHB. So for Cal and Xan in the aqueous phase, it is 10.02 and 10.69 kcal/mol lower, respectively. This is due to the reduction of the IMHB process in water, and the carbonyl and hydroxy functional groups form intermolecular hydrogen bonding with water. Antioxidants can also prevent the destructive action of a free radical using the SET-PT mechanism. The antioxidant is converted to a radical cation (reaction (4)). The most crucial factor that affects the IP value of an antioxidant is the extended delocalization of electron spin density and positive charge through the resonance process. IP data and ΔIP values for Cal, Xan, and phenol at the computational level of B3LYP/6–31 + G (d, p) have been presented in Table 4. The IP of both flavonoids is less than phenol, with positive values ΔIP. IP for Cal in water is 6.98 kcal/mol lower than Xan. Both flavonoids based on IP data are effective antioxidants. According to Fig. 2S, radical cation $Cal^{\circ+}$ and $Xan^{\circ+}$ show the spin density distribution more on ring A and ring C. MEP maps also show a positive charge on ring A. Three methoxy substitutions stabilize the positive charge (Supplementary material).

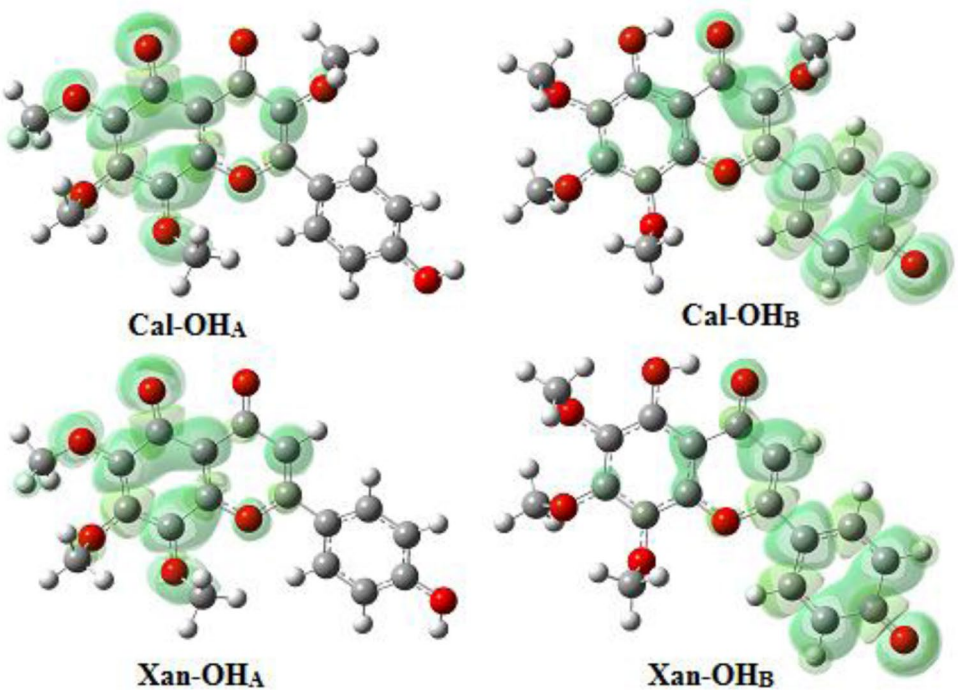

Fig. 4 Maps of spin density for various radicals of calycopterin and xanthomicrol in water

As mentioned above, the value of IPs can be obtained from the enthalpy changes of reaction (8). Negative HOMO energy levels can also be used for antioxidant investigation. Accordingly, the HOMO orbital energy in water for Cal and Xan phenols is 6.90, 6.11, and 6.20 eV, respectively and, these numbers show that Cal is a more robust antioxidant than the rest. The enthalpy calculations of reaction (8) also confirm this result. The IP values for Cal are 11.40 and 6.98 eV lower than phenol and Xan in water, respectively. This arrangement is better seen in the gas phase (Table 4). It is worth noting that the SET-PT mechanism is highly dependent on the polarity of the environment. Findings have also been reported in the literature so that the SET-PT mechanism performs better in polar solvents such as water and has lower energy than the gas phase [67]. As can be deduced from IP data, the loss of an electron and the formation of a radical cation in water are more favorable for phenol, Cal, and Xan as 51.73, 56.19, and 72.89 kcal/mol, respectively, than for the gas phase. The reason for this is the solvation of radical cation in the polar solvent.

Another mechanism reported for the action of antioxidants in sources is the sequential proton loss electron transfer (SPLET) mechanism (reaction (7)):

3. Sequential proton loss electron transfer (SPLET):

$$ArOH \rightleftharpoons ArO^- + H^+; \quad ArO^- \rightarrow ArO^{\bullet} + e \tag{7}$$

As seen from reaction (7), the first step is the deprotonation of the antioxidant and the formation of the ArO^- anion, which then converts to an ArO° radical by losing one electron. The first step is in an equilibrium state, and the more stable conjugate base results in the strong acid of ArOH. As a result, its antioxidant properties will improve. Therefore, the proton affinity (PA) values at 298.15 K in the gas phase were calculated as -ΔH of reaction (8) using Eq. (9).

$$ArO^- + H^+ \rightarrow ArOH \tag{8}$$

$$PA = -\Delta H = H_{ArO^-} + H_{H}{}^{+} - H_{ArOH} \tag{9}$$

As seen in Table 4, the values of PAs are significantly lower than BDEs and IPs. Therefore, from a thermodynamic point of view, the first stage of the SPLET (Deprotonation) mechanism is more desirable in the studied structures. On the other hand, the PA values of Cal-OH_B and Xan-OH_B groups are lower and more acidic than the hydroxy group of ring A and also phenol, which is due to the stability of the resulting anion (ArO^-) through negative charge delocalization by ring B and pyrone ring (Scheme 2).

Table 5 The calculated structural data of anions of Cal-OH_B and Xan-OH_B by B3LYP/6–31 + G(d, p) method

Parameter	Value[a]	
	Cal-OH_B	**Xan-OH_B**
IMHB[b] length (Å)	1.631 (1.586)	1.625 (1.578)
IMHB angle (°)	152.10 (153.34)	152.39 (153.62)
C = O bond length (Å)	1.277 (1.276)	1.274 (1.274)
C_B–C_C bond length[c] (Å)	1.445 (1.429)	1.441 (1.427)

[a]In parenthesis for the gas phase

[b]IMHB: intramolecular hydrogen bond

[c]bond between rings B and C

The negative charge delocalization makes the IMHB bond stronger in the anion than in the neutral form. Comparison of the data in Table 5 with Table 1 confirms that the length of IMHB in the resulting anions is shorter and the bond angle is increasing and reaching a linear state. It is worth mentioning that the IMHB is stronger in the more linear case [68]. The bond length of the carbonyl group in Cal-OH_B and Xan-OH_B anions is longer than in the neutral state and the C_B–C_C bond length in the anion is shorter than in the neutral state (Tables 5 and 1), all of which indicate the negative charge distribution in the conjugate system of rings B and C. MEP maps also show the placement negative charge on rings B and C as well as the carbonyl group (Fig. 3S, supplementary material).

The oxygen radicals are active and reactive radical species produced by various biological processes in the human body and must be neutralized and eliminated with antioxidants. In order to have a deeper understanding of the ability of Cal and Xan to scavenge oxygen radicals (OH°, HOO°, and $O_2^{\circ-}$), the reaction of Cal and Xan with these active species using the computational method B3LYP/6–31 + G(d, p) was studied. These reactive oxygen radicals can separate a hydrogen atom from the flavonoid and form a new radical

Scheme 2 Stabilization of anion of Cal-OH_B by resonance

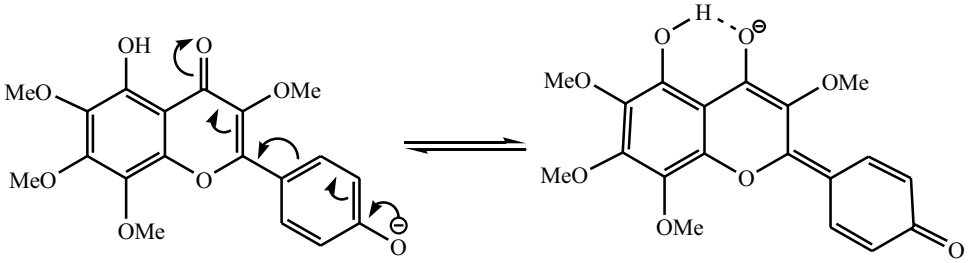

anion of Cal-OH_B

Table 6 The Gibbs free energies (ΔG) for the interaction of calycopterin and xanthomicrol with HO˚, HOO˚, and $O_2^{\circ-}$ calculated by B3LYP/6–31 + G(d, p) method[a]

Structure	ΔG_{OH°	ΔG_{OOH°	$\Delta G_{O2^{\circ-}}$
Phenol	–39.00 (36.07)	–4.29 (2.47)	15.17 (19.45)
Cal-OH$_A$	–31.5 (21.64)	3.40 (11.96)	19.85 (33.73)
Cal-OH$_B$	–35.68 (34.26)	–0.74 (0.65)	16.40 (21.27)
Xan-OH$_A$	–29.97(20.06)	4.45(13.53)	21.59 (35.46)
Xan-OH$_B$	–33.99(32.90)	0.43(0.69)	17.57(22.62)

[a]In parenthesis for the gas phase

species that are more stable and less reactive (reactions (10)–(12)).

$$ArOH + HO^{\bullet} \rightarrow ArO^{\bullet} + H_2O \quad (10)$$

$$ArOH + HOO^{\bullet} \rightarrow ArO^{\bullet} + H_2O_2 \quad (11)$$

$$ArOH + O_2^{\bullet-} \rightarrow ArO^{\bullet} + HOO^{-} \quad (12)$$

The Gibbs free energies (ΔGs) of these reactions in water and the gas phase have been given in Table 6. The reaction of the studied compounds with OH˚ is an exothermic reaction and ΔG_{OH° is between 39.00 and 29.97 kcal/mol. In general, hydroxy groups on Cal have a higher trapping ability than Xan hydroxy groups (Table 6). The reaction of the OH_B group with the OH˚ radical releases more heat than the OH_A group, which is in complete agreement with the data obtained from the antioxidant properties of the mechanisms discussed above.

As can be seen from the data in Table 6, ΔG for HOO˚ radical reactions is almost endothermic, except for the hydroxy OH_B group in the Cal compound. The reaction of all active sites in the compounds Cal and Xan with $O_2^{\circ-}$ is endothermic and the free energy in water is between 16.40 and 35.46 kcal/mol. These results indicate that the OH˚ radical is the most active species for abstraction of the hydrogen radical atom from Cal and Xan. On the other hand, the reactivity of the OH_B group with reactive oxygen radicals is the highest.

Conclusions

In this study, for the first time, two valuable flavonoids with high biological properties (Cal and Xan) are comprehensively studied by computational method B3LYP/6–31 + G(d, p) to obtain structural and electronic information in the gas phase as well as water. The computational method was evaluated using ^{1}HNMR and ^{13}CNMR experimental data, and there was excellent agreement between computational and experimental chemical shifts. The optimized structure of these compounds shows the presence of strong intramolecular hydrogen bonds, which incidentally strongly affect their physical and chemical properties, including antioxidant properties. Acceptable aromaticity is seen in the pyrone ring, which was evaluated by HOMA and NICS indices. Calculation and data analysis on electron properties (HOMO and LUMO) and reactivity (electrophilicity and nucleophilicity indices) show that Cal has higher reactivity than Xan. In the last part of this study, the antioxidant properties of these compounds with different mechanisms in the gas and water phases were comprehensively investigated. The results show that these flavonoids have good antioxidant properties. The main reason for this property is the stability of radicals produced by the conjugate system in their structure. The presence of the methoxy as an electron donor group on the pyrene ring of Cal makes its antioxidant properties higher than Xan. Examination of the reactivity of the studied compounds with oxygen radicals showed that a possible reaction to abstract the hydrogen radical from these compounds will occur by OH˚. Given the dependence of antioxidant properties on lipophilicity, the lipophilicity index of these compounds was also calculated and the results confirmed that Cal is more lipophilic than Xan.

Supplementary information The online version contains supplementary material available at https://doi.org/10.1007/s11224-022-01929-9.

Author contribution Arjang Jalezadeh: formal analysis, investigation, resources, software, validation, visualization. Zohreh Mirjafary: conceptualization, formal analysis, investigation, resources, software, validation, visualization, writing- review and editing. Morteza Rouhani: advising, writing- review and editing. Hamid Saeidian: conceptualization, formal analysis, investigation, resources, software, validation, visualization, writing—review and editing.

Availability of data and material The online version of this article contains supplementary material, which is available to authorized users.

Declarations

Conflict of interest The authors declare no competing interests.

References

1. Leopoldini M, Russo N, Toscano M (2011) Food Chem 125:288
2. Montané X, Kowalczyk O, Reig-Vano B, Bajek A, Roszkowski K, Tomczyk R, Pawliszak W, Giamberini M, Mocek-Płóciniak A, Tylkowski B (2020) Molecules 25:3342
3. Garcia-Lafuente A, Guillamon E, Villares A, Rostagno M, Martinez J (2009) Inflamn. Res 58:537
4. Abbas M, Saeed F, Muhammad F, Afzaal M, Tufail T, Bashir MS, Ishtiaq A, Hussain S, Suleria HAR (2017) Int J Food Prop 20:1689
5. Abotaleb M, Samuel SAM, Varghese E, Varghese S, Kubatka P, Liskova A, Busselberg D (2019) Cancers 11:28
6. Stuetz W, Prapamontol T, Hongsibsong S (2010) J Agric Food Chem 58:6069

7. Pereira CV, Duarte M, Silva P, Silva AB, Duarte CMM, Cifuents A, Albuquerque C, Teresaserra A (2019) Nutrients 11:326
8. Karrer W, Venkataraman K (1935) Nature 135:878
9. Ratnagiriswaran AN, Sehra KB, Venkataraman K (1934) Biochem J 28:1964
10. Farimani MM, Sarvestani N, Ansari N, Khodagholi F (2011) Chem Res Toxicol 2280
11. Esmaeli MA, Farmani MM, Kiaei M (2014) Mol Cell Biochem 397:17
12. Lotfizadeh R, Sepehri H, Attari F, Delphi L (2020) Iran J Pharm Res 19:391
13. Faham N, Javidani K, Bahmani M, Amirghofran Z (2008) Phytother Res 22:1154
14. Moghaddam GH, Ebrahimi SA, Rahbar-Roshandel N, Foroumadi A (2012) Phytother Res 26:1023
15. Abbaszadeh H, Ebrahim SA, Akhavan MM (2014) Phytother Res 28:1661
16. Ghazizadeh F, Shafiei M, Falak R, Panahi M, Rakhshani N, Ebrahimi SA, Moghaddam PR (2020) Evid Based Complement Alternat Med 2020:1
17. Fattahi M, Cusido RM, Khojasteh A, Bonfill M (2014) J Palazon Med Chem 14:725
18. Attari F, Keighobadi FK, Abdollahi M, Arefian E, Lotfizadeh R, Sepehri H, Farimani MM (2021) Phytother Res 35:1967
19. Lobo V, Patil A, Phatak A, Chandra N (2010) Pharmcogn Rev 4:118
20. Carocho M, Ferreira ICFR (2013) Food Chem Toxicol 51:15–25
21. Ebrahimzadeh MA, Khalili M (2015) J Mazandaran Univ Med Sci 24:188
22. Lu JM, Lin PH, Yao Q, Chen C (2010) J Cell Mol Med 14:840
23. Cadenas E (1998) Mechanisms of Antioxidant Action. In: T. Özben T. (eds) Free Radicals, Oxidative Stress, and Antioxidants. NATO ASI Series (Series A: Life Sciences), Springer, Boston, MA 296
24. Javan AJ, Javan MJ (2014) Food Chem 165:451
25. Tajammal A, Siddiqa A, Irfan A, Azam M, Hafeez H, Munawar MA, Basra MA (2021) Mol Struct 1254 132189
26. Ivanova A, Gerasimova E, Gazizullina E (2020) Molecules 25:4251
27. Wang F, Ye S, Ding Y, Ma Z, Zhao Q, Zang M, Li Y (2022) Mol Struct 1252:132185
28. Shi Y (2021) Sci Rep 11:8806
29. Shatokhin SS, Tuskaev VA, Gagieva SC, Markova AA, Pozdnyakov DI, Melnikova EK, Bulychev BM, Oganesyan ET (2021) J Mol Struct 1249:131683
30. Wang MY, Ma ZL, He CL, Yuan XY (2020) Nat Prod Res 20:1
31. Sholl DS, Steckel JA (2009) Density functional theory: a practical introduction. John Wiley & Sons Inc
32. Burke K (2012) J Chem Phys 136:150901
33. Rouhani M (2021) Comput Theor Chem 1195:113096
34. Javan AJ, Javan MJ, Tehrani ZA (2013) J Agric Food Chem 61:1534
35. Ngo TC, Dao DQ, Nguyen MT, Nam PC (2017) RSC Adv 7:39686
36. Chen K, Shang Y, Zhou H, Li X, Zhou J (2019) New J Chem 43:15736
37. Hernandez DA, Rodriguez-Zavala JG, Tenorio FJ (2020) Struct Chem 31:359
38. Leopoldini M, Marino T, Russo N, Toscano M (2004) J Phys Chem 108:4916
39. Esmaeili A, Mohabi N (2014) Int J Food Prop 17:1162
40. Sonam CV, Kakkar R (2020) Struct Chem 31:1599
41. Frisch MJ, Trucks GW, Schlegel HB, Scuseria GE, Robb MA, Cheeseman JR, Zakrzewski VG, Montgomery JA, Stratmann RE Jr, Burant JC, Dapprich S, Millam JM, Daniels AD, Kudin KN, Strain MC, Farkas O, Tomasi J, Barone V, Cossi M, Cammi R, Mennucci B, Pomelli C, Adamo C, Clifford S, Ochterski J, Petersson GA, Ayala PY, Cui Q, Morokuma K, Salvador P, Dannenberg JJ, Malick DK, Rabuck AD, Raghavachari K, Foresman JB, Cioslowski J, Ortiz JV, Baboul AG, Stefanov BB, Liu G, Liashenko A, Piskorz P, Komaromi I, Gomperts R, Martin RI, Fox DJ, Keith T, Al-Laham MA, Peng CY, Nanayakkara A, Challacombe M, Gill PMW, Johnson BG, Chen W, Wong MW, Andres JL, Gonzalez C, Head-Gordon M, Replogle ES, Pople JA, Gaussian 09 (2013) Gaussian, Inc., Wallingford
42. Saeidian H, Babri M, Sharifi DA, Sarabadani M, Naseri MT (2013) Anal Bioanal Chem 405:6749
43. Makkara P, Ghosh NN (2021) RSC Adv 11:27897
44. Kapil J, Shukla P, Pathak A (2020) Review article on density functional theory. In: V. K. Jain, S. Rattan, A. Verma, Recent trends in materials and devices, Springer, Singapore. Proceedings in Physics 256
45. Saeidian H, Shams B, Mirjafary Z (2019) Struct Chem 30:787
46. Morgante P, Peverati R (2020) Int J Quantum Chem 120:26332
47. Saeidian H, Mirjafary Z (2020) New J Chem 44:12967
48. Paghandeh H, Foumeshi MK, Saeidian H (2021) Struct Chem 32:1279
49. Takano Y, Houk KN (2005) J Chem Theor Comput 1:70
50. Wolinski K, Hinton JF, Pulay P (1990) J Am Chem Soc 112:8251
51. Krygowski TM, Szatylowicz H, Stasiuk OA, Dominikowska J, Palusiak M (2014) Chem Rev 114:6383
52. Gershoni-Poranne R, Stanger A (2015) Chem Soc Rev 44:6597
53. Raczynska ED, Hallman M, Kolczynska K, Stepniewski TM (2010) Symmetry 2:1485
54. Raczynska ED, Gal JF, Maria PC, Saeidian H (2021) Symmetry 13:1554
55. Chen Z, Wannere CS, Corminboeuf C, Puchta R, Schleyer PVR (2005) Chem Rev 105:3842
56. Murray SJ, Politzer P (2011) Wires 1:153
57. Weinhold F, Landis CR, Glendening ED (2016) Int Rev Phys Chem 35:399
58. Rajan VK, Muraleedharan K (2017) Food Chem 230:93
59. Young DC (2001) Computational chemistery a practical guide for applying techniques to real-word problem. John Wiley & Sons Inc. 9
60. Chattaraj PK, Giri S, Duley S (2011) Chem Rev 111:43
61. Perez P, Domingo LR, Aizman A, Contreras R, Labbe AT (2007) Theor. Comput Chem 19:139
62. Domingo LR, Gatierrez MR, Perez P (2016) Molecules 21
63. Jaramillo P, Domingo LR, Chamorro E, Perez P (2008) J Mol Struct 865:68
64. Domingo LR, Perez P, Ortega DE (2013) J Org Chem 78:2462
65. Daina A, Michielin O, Zoete V (2017) Sci Rep 7:42717
66. Szeląg M, Urbaniak A, Bluyssen HAR (2015) Open Chem 13:17
67. Wright JS, Johnson ER, Di Labio GA (2001) J Am Chem Soc 123:1173
68. Bachrach SM, Wilbanks CC (2010) J Organomet Chem 75:2651